Multiple molecular events determine stochastic cell fate switching in a eukaryotic bistable system

Naomi Ziv[1], Lucas R. Brenes[1,2], Alexander Johnson[1]

[1]Department of Microbiology and Immunology, University of California, San Francisco
[2]Present Address: Biology Graduate Program, Massachusetts Institute of Technology

Eukaryotic transcriptional networks are often large and contain several levels of feedback regulation. Many of these networks exhibit bistability, the ability to generate and stably maintain two distinct transcriptional states and to switch between them. In certain instances, switching between cell states is stochastic, occurring in a small subset of cells of an isogenic population in a seemingly homogenous environment. Given the scarcity and unpredictability of switching in these cases, investigating the determining molecular events is challenging. White-opaque switching in the fungal species *Candida albicans* is a complex bistable eukaryotic system and can serve as an experimentally accessible model system to study characteristics important for bistability and stochastic cell fate switching. In standard lab media, switching is rare, and genetically identical cells maintain their cellular identity (either "white" or "opaque") through thousands of cell divisions. By isolating populations of white or opaque cells and measuring switching frequencies, previous studies have elucidated the many differences between the two cell states and identified a set of transcriptional regulators needed for cell type switching. Yet little is known about the molecular events that determine the rare, stochastic switching events that occur in single cells. We use microfluidics combined with fluorescent reporters to directly observe rare switching events between the white and opaque states. We investigate the stochastic nature of switching by beginning with white cells and monitoring the activation of Wor1, a master regulator and marker for the opaque state, in single cells and throughout cell pedigrees. Our results indicate that switching requires two stochastic steps; first an event occurs that predisposes a lineage of cells to switch. In the second step, some but not all, of those predisposed cells rapidly express high levels of Wor1 and commit to the opaque state. To further understand the rapid rise in Wor1, we used a synthetic inducible system in *Saccharomyces cerevisiae* into which a controllable *C. albicans* Wor1 and a reporter for its transcriptional control region have been introduced. We document that Wor1 positive autoregulation is highly cooperative (Hill coefficient > 3), leading to rapid activation and producing an "all or none" rather than a graded response. Taken together, our results suggest that reaching a threshold level of a master regulator is sufficient to drive cell type switching in single cells and that an earlier molecular event increases the probability of reaching that threshold in certain small lineages of cells. Quantitative molecular analysis of bistability in the white-opaque circuit can serve as a model for the general understanding of complex circuits.

Introduction

Transcription circuits, defined as transcription regulators and the DNA cis-regulatory sequences they bind, control the expression of genes and thereby define cellular identity. Cellular identity is not static; gene expression programs change in response to external and internal stimuli. Certain transcriptional networks can exhibit bistability, in which a biological system can toggle between two stable states. The best-characterized bistable circuits come from microbes, such as the cI-Cro circuit of phage lambda (Ptashne, 2011), the control of lactose utilization in *Escherichia coli* (Santillán & Mackey, 2008), competence in *Bacillus subtilis* (Maamar & Dubnau, 2005) and galactose utilization in *Saccharomyces cerevisiae* (Stockwell et al., 2015). Bistability has also been engineered in both prokaryotic and eukaryotic synthetic circuits (Gardner et al., 2000; Kramer et al., 2004; Wu et al., 2013) and is thought to underlie many instances of cell differentiation in multicellular organisms (Chickarmane et al., 2006; Graham et al., 2010; Park et al., 2012). The emergence of bistability depends on the presence of positive feedback regulation and non-linearity (such as cooperativity) within the feedback circuit, which can convert graded inputs into discontinuous switch-like outputs (Alon, 2007; Ferrell, 2002; Smits et al., 2006). The output of a given circuit "diagram" however, is entirely dependent on the physical parameters of the components, such as dissociation constants and protein concentrations; even slight variations in circuit architecture or parameters can produce distinct outputs (Çağatay et al., 2009). Many questions remain concerning the functional properties and parameters of network motifs found in real biological systems, particularly those based on the large regulatory networks commonly found in eukaryotic organisms. A major challenge to experimentally investigating the functional role of the multiple feedback loops present in complex circuits is the limited ability to independently manipulate the different components. In order to understand the output of these large networks, it is necessary to integrate the analysis of individual motifs with an analysis of the network as a whole.

In some cases, switching between states depends on external signals, but in other cases switching between stable states appears stochastic, occurring in a subset of cells of an isogenic population in a seemingly homogenous environment. In microbes, stochastic phenotypic switching is often thought of in terms of adaptation to fluctuating environments (Acar et al., 2008; Kussell, 2005b), where there is a predicted optimal relationship between the frequency of stochastic switching and the frequency of environmental change. In pathogens, stochastic switching can create distinct subpopulations with different cell features, protecting against targeted host defense systems (Norman et al., 2015). Stochastic switching also occurs during development to create cellular diversity (Losick & Desplan, 2008). For example, photoreceptor patterning in the fly retina is based on a choice between cell states following the stochastic expression of a single transcription factor (Wernet et al., 2006). Understanding stochastic phenotype switching at a molecular level is challenging, in particular, identifying the early, seemingly random, initiating events that determine which cells will undergo switching.

To study the mechanism of stochastic switching between two stable transcription states, we investigate white-opaque switching in *Candida albicans*, a common component of the human gut microbiota but also an opportunistic pathogen causing life-threatening bloodstream infections (Kim & Sudbery, 2011). White and opaque cells differ in the expression of hundreds of genes resulting in drastic differences in cell morphology, metabolism, the ability to mate and interactions with the immune system (Ene et al., 2016; Lohse & Johnson, 2009; Miller & Johnson, 2002; Sasse et al., 2013; Tuch et al., 2010). A complex transcriptional network controls white-opaque switching, as many (at least seven) transcription factors are involved and are known to regulate one another, in a series of nested feedback loops (Hernday et al., 2013; Lohse et al., 2016; Zordan et al., 2007). The master regulator of white-opaque switching is Wor1, a transcription factor whose deletion disables switching (locking cells in the white state) and whose ectopic expression in white cells converts them *en masse* to opaque cells, even in the absence of other critical regulators (Lohse & Johnson, 2016; Zordan et al., 2006, 2007). Wor1 is differently regulated between the two cell states, with 40-fold higher expression in opaque cells. In common with the other regulators of white-opaque switching, the Wor1 regulatory sequences (7KB upstream control region and 2KB 5'UTR) are some of the longest in the *C. albicans* genome (Tuch et al., 2010). Its complexity is reminiscent of enhancers from multicellular organisms, even exhibiting the phase transitions described for some mammalian enhancers (Frazer et al., 2020). Wor1 is positioned in the center of a network of multiple positive feedback loops, binding both its own promoter as well as those of both activators and repressors of the opaque cell state (Hernday et al., 2013; Zordan et al., 2007).

In this work, we investigate the process of white-opaque switching at a single cell level. To do so, we developed two complementary quantitative approaches to study the molecular mechanisms underlying switching. The first is the use of microfluidics and fluorescent microscopy to follow switching in *C. albicans*, allowing us to quantify the activation of the master regulator Wor1 in pedigrees where both switching and non-switching cells are dividing. The second is the use of a synthetic inducible system in *S. cerevisiae* to investigate the function of white-opaque regulators and characterize specific regulatory interactions, such as Wor1 autoregulation. Our results reveal features of white-opaque switching that were unanticipated from previous "bulk" culture analyses and provide key insights into the mechanism behind stochastic switching.

Results

Observing white-opaque switching at a single cell level

White-opaque switching has typically been studied by monitoring the formation of colony sectors after plating single cells on solid agar and allowing them to grow and form colonies of approximately 10^6 cells (FIGURE 1A, 1B, TABLE S1). A sector registers a switching event that took place in the past and reveals the stochastic nature of switching (e.g. sectors of different sizes in different colonies) but provides no insight into how the original cell that founded the sector differed from the surrounding cells and underwent switching. We set out to observe switching at a single cell level to understand how this process occurs. Using switching competent *C. albicans* a/Δ diploid cells (METHODS), we took advantage of microfluidic plates that contain specialized barrier traps (FIGURE 1C, METHODS). As the experiment begins, traps contain a few cells and, over time, these cells divide, eventually filling the trap. After approximately 12 hours, each trap holds ~400 cells. We continue imaging cells for an additional 12 hours, during which cells continue to divide in the trap, pushing excess cells out of the trap where they flow away. With this experimental set-up, we are able to observe thousands of divisions in each trap and, by monitoring many traps, capture detailed instances of stochastic white-opaque switching, even though these events are rare.

Wor1 is a master regulator of white-opaque switching and its expression is 40-fold higher in opaque cells compared to white cells (Zordan et al., 2006). We followed switching events in a strain homozygous for a Wor1-GFP fusion protein (FIGURE 1D, VIDEO 1). Microfluidic experiments that began with cells from white colonies did not have any visible GFP signal while those that began with cells from opaque colonies had uniformly high levels of GFP signal (FIGURE 1D, FIGURE S1). Using this strain allowed for the unambiguous identification of switching events as well as the quantification of the increase in Wor1 expression as cells transition between the white and opaque states. Although switching is still relatively rare and stochastic, strains containing the Wor1-GFP fusion switch at higher rates than wildtype cells (TABLE S1), which enabled observation of many independent switching events. GFP is known to form dimers at high concentrations (Phillips, 1997; Yang et al., 1996) and when we introduced the GFP A206K mutation (differentiated as mGFP below) to prevent dimerization (Zacharias, 2002), white-opaque switching reverted to wildtype levels (TABLE S1). By visualizing a large number of traps, we were able to observe several switching events in the Wor1-mGFP fusion strain. Apart from the difference in switching frequency, the switching behavior (as described below) of the Wor1-mGFP fusion strain appeared identical to the Wor1-GFP strain. Most of our data therefore was obtained from the elevated switching strain with the low-switching strain used to validate it. As predicted from previous bulk culture experiments, once the Wor1-GFP fusion reached a high level, it was faithfully passed on to descendent cells, preserving the opaque state.

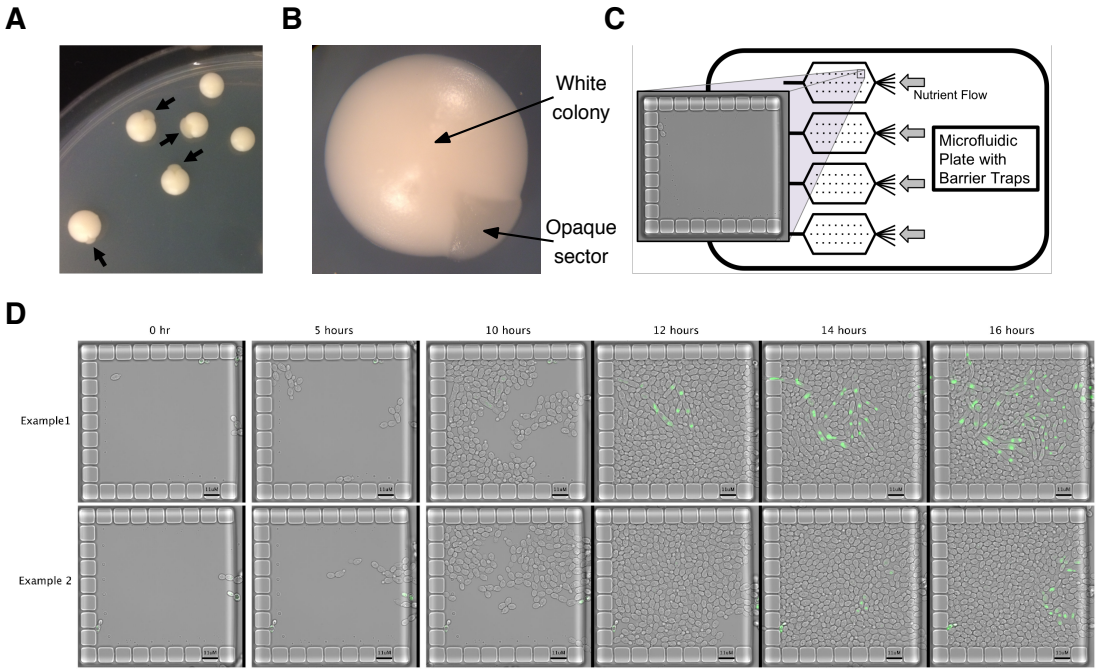

FIGURE 1 legend – Monitoring white-opaque switching in *Candida albicans*
A) Image of colonies produced by plating single white cells on solid agar. Arrows point to opaque sectors; each represents an independent switching event. This strain contains the Wor1-GFP fusion protein and hence exhibits higher than normal switching rates. B) Close up image of single white cell type colony with an opaque sector. C) Schematic of microfluidic plates used to study white-opaque switching at a single cell level. Each plate has four chambers; each chamber contains 104 barrier traps. D) Two examples of microfluidic traps in which a switching event occurred. The strain contains the Wor1-GFP fusion protein and cells enter the trap (from the right) as white cells. As cells complete switching to the opaque state, the Wor1-GFP fusion reaches high levels of expression.

VIDEO 1 legend – Example of time-lapse movie of a switching event
Movie corresponds to 'Example 1' in FIGURE 1D. Movie is shown twice; in the second repetition, tracked cells are labeled. This strain contains the Wor1-GFP fusion protein.

Observations on pseudohyphal growth and mitosis

Consistent with a previous report (Bergen et al., 1990), we observed elongated cells reminiscent of pseudohyphae (Sudbery et al., 2004) as intermediates in some instances of white-opaque switching. Typically a round mother cell buds an elongated cell and both subsequently activate Wor1 (FIGURE 2, FIGURE S2). It is possible that pseudohyphal formation increases the probability of switching; however, it is not necessary or sufficient for switching as we observed pseudohyphal formation without switching and switching without pseudohyphal formation. In the majority of cases, descendents of initial

194 switching cells resemble typical opaque cells (which are slightly more elongated than
195 white cells) within a few cell divisions.
196

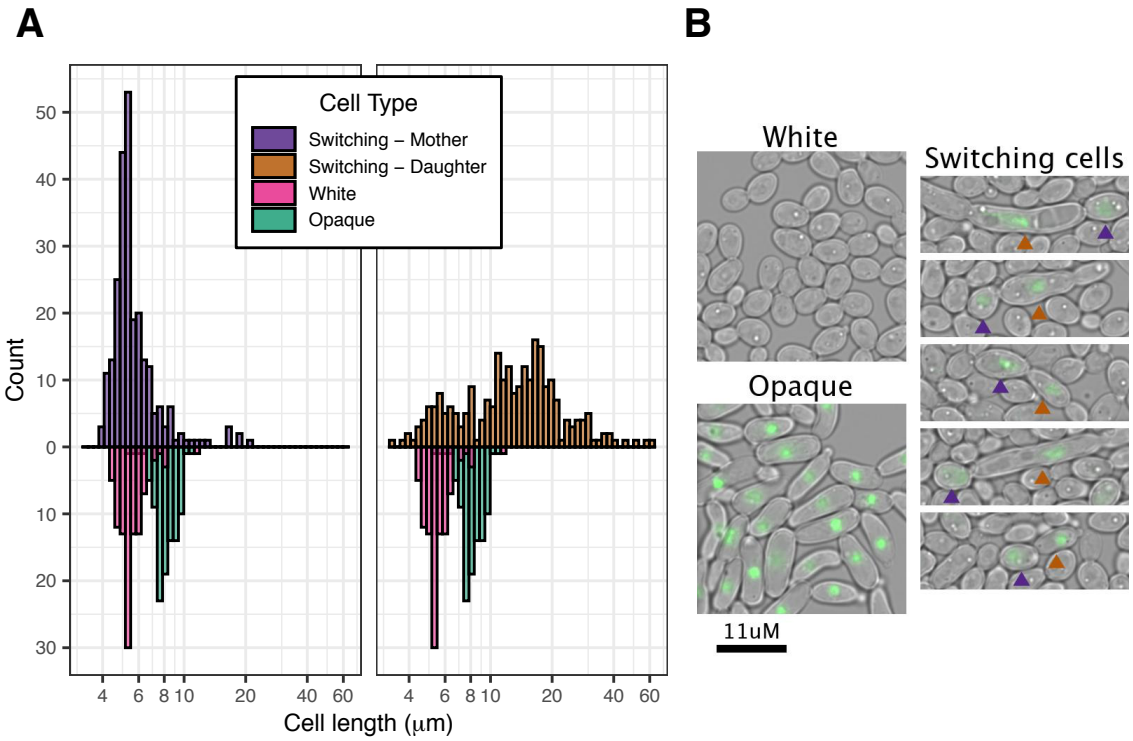

197
198
199 FIGURE 2 legend – Cell length distribution of switching cells
200 A) Cell length distribution of switching cells compared to typical white and opaque cells.
201 Switching initiates in pairs of mother and daughter cells, the left histogram shows the size
202 distribution for mothers, the right, for daughters. Typical white and opaque cell
203 distributions are shown beneath each histogram for reference. The strain contains the
204 Wor1-GFP fusion protein. X-axis is logarithmic B) Representative images of white,
205 opaque and cells undergoing white to opaque switching. Arrows point out mother and
206 daughter in each switching pair with colors corresponding to (A). Although elongated
207 (pseudohyphal) cells are observed, they are neither necessary nor sufficient for switching.
208
209 Although not a primary goal of this work, the nuclear localization of Wor1 allowed us to
210 observe certain features of mitosis in switching cells. In a subset of cases, nuclear
211 division occurred within the elongated daughter cell and not across the bud neck
212 (FIGURE S3). Similar observations have been seen in filamentous forms of *C. albicans*
213 (Sudbery et al., 2004). In some of our examples, one of the two nuclei in the daughter cell
214 returned to the mother cell and both cells continued dividing (FIGURE S3A). In other
215 examples, both nuclei remained in the elongated daughter forming polyploid cells
216 (FIGURE S3B). In these cases, the mother cell no longer divided. This distinctive mitosis
217 pattern did not always occur during switching and, as a result, the majority of opaque
218 cells are not polyploid. Although we were able to observe these deviations from
219 conventional mitosis, they are not required for switching, as we did not observe them in

all switching events. Furthermore, these atypical mitosis events are likely specific to *C. albicans* cells and do not represent a general feature of bistable systems.

WOR1 activation is synchronous in mother-daughter pairs and is stereotypical across independent switching events

To quantify switching, we developed a custom semi-automated image analysis pipeline to measure Wor1-GFP (or Wor1-mGFP) levels in single cells over time (FIGURE S4, METHODS). Because Wor1 is nuclear localized, we used the average of the 300 highest intensity pixels per cell as a quantitative measure of Wor1 levels. During switching, Wor1 levels increase and then oscillate in concert with nuclear divisions similar to those observed in established opaque cells (FIGURE 3A). Comparing Wor1 activation in mother cells of independent switching events (taken from different traps and experiments) reveals a generally stereotypical response (FIGURE 3B) taking approximately three hours to reach maximum Wor1 levels. Consistent with the stochastic nature of switching, the starting time of different switching events did not depend on the time (or number of cell divisions) from the beginning of the experiment. Moreover, even the time between the birth of a switching cell and its switching varies from one cell to the next.

As mentioned above, Wor1 activation occurs in dividing cells where both mother and daughter cells typically activate Wor1 simultaneously. This synchronous activation at times extends to the mother cells' previous daughter as well, leading to four cells (mother, two daughters and one granddaughter) activating Wor1 simultaneously (FIGURE 3C, 3D). The synchrony in Wor1 activation between mother and daughter cells suggest the pace of Wor1 activation is determined early in the switching event. Once high levels of Wor1 were reached, they were always inherited across subsequent cell divisions indicating that the switch was complete.

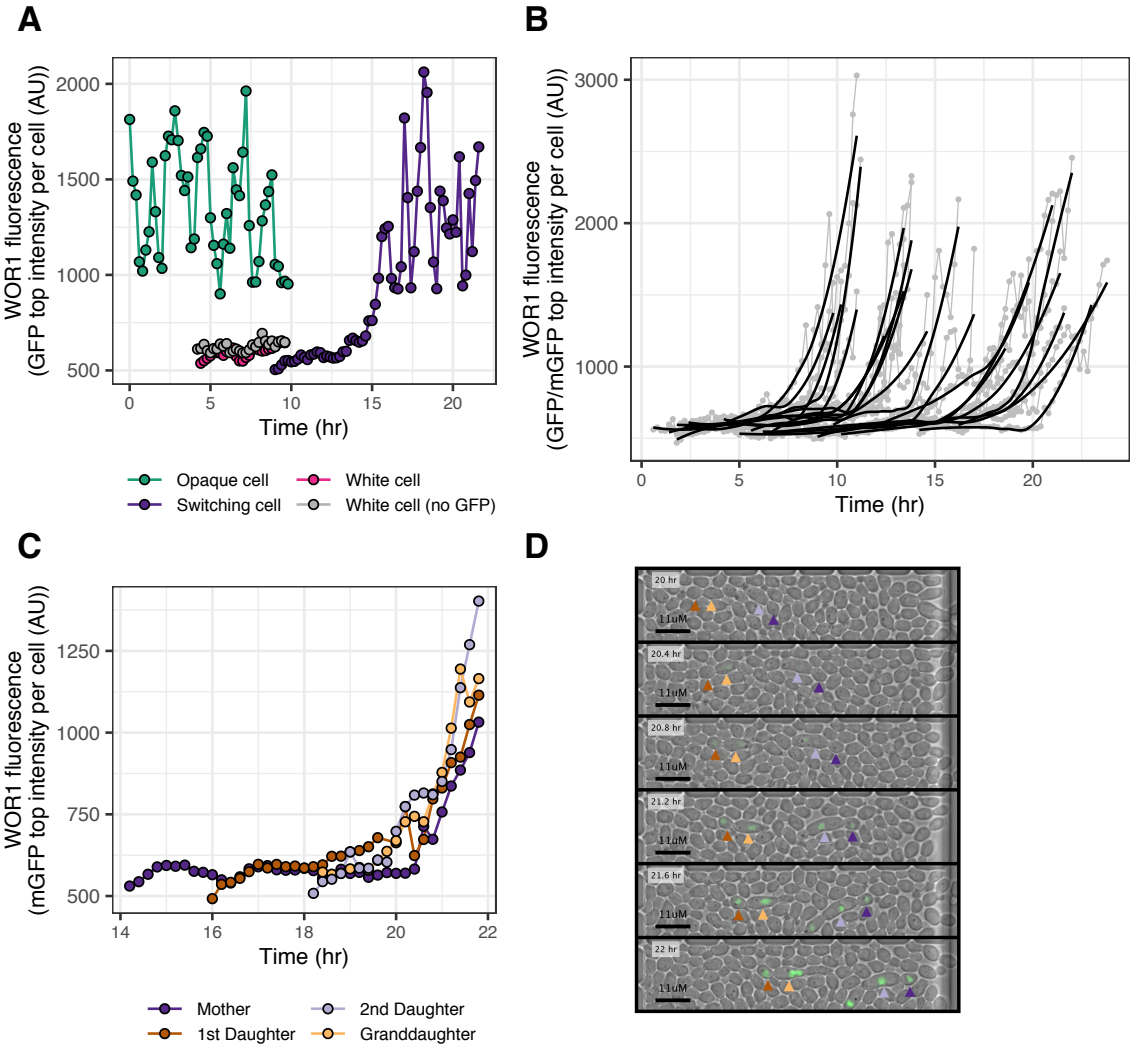

FIGURE 3 legend – Wor1 fluorescence (GFP/mGFP) levels in single cells
A) Representative example of a Wor1 expression level trace in a single switching cell (purple). Traces of typical white (pink) and opaque (green) cells are shown for reference. Oscillations in high Wor1 levels occur with nuclear divisions. X-axis represents time from the beginning of the experiment; examples are taken from cells born at different times. The strain contains the Wor1-GFP fusion protein. B) Examples of Wor1 activation in single switching cells. Traces (grey points and lines) are truncated to highlight the initial activation of Wor1. Black lines represent locally estimated scatter-plot smoothing (LOESS) of individual traces. Examples are taken from three different experiments, representing strains containing the Wor1-GFP (n=17) or the Wor1-mGFP (n=4) fusion protein. C) Representative example of a four-cell (direct mother-daughter) pattern of synchronous Wor1 activation. X-axis represents time from the beginning of the experiment and traces are shown starting at the birth of the mother cell. The strain contains the Wor1-mGFP fusion protein. D) Subset of images representing data shown in (C) with time proceeding from top to bottom. Arrows point to individual cells with colors corresponding to (C). All four switching cells simultaneously activate Wor1.

Certain lineages of cells show unusual switching patterns

An unanticipated feature of white-opaque switching emerged when we reconstructed complex pedigrees of switching cells, tracing the prior histories of cells destined to switch. In addition to the simple pairs of mother-daughter cells activating Wor1 simultaneously described above, we observed instances where additional cells in the same trap also activated Wor1. Pedigree analysis revealed that these additional cells were closely related to the conventional mother-daughter switching pairs, through a previous mother, daughter or sister (FIGURE 4A). However, these related switching cells were separated by cell divisions that produced cells that did not switch, creating small mixed-fate pedigrees (FIGURE4A).

To determine if these cases are the result of entirely independent switching events or are due to a complex pattern of switching within a single linage, we analyzed the Wor1-mGFP strain, where overall switching rates are lower. We estimate the Poisson probability distribution for multiple switching events per trap based on the proportion of traps where there was no Wor1 activation (134/168 traps) (FIGURE 4B, METHODS). We find that the Poisson expectation (FIGURE 4B, white bars) of switching events is matched exactly when considering direct mother-daughter and mixed-fate pedigrees as single dependent switching events (Chi-squared goodness of fit p-value, 0.986), (FIGURE 4B, light grey bars). However, the expectation is not matched if direct mother-daughter pedigrees are considered dependent but mixed-fate pedigrees are considered two independent events (Chi-squared goodness of fit p-value, 0.0034), (FIGURE 4B, medium grey bars). This analysis rules out multiple independent events as the explanation for mixed-fate pedigrees and indicates that the switching events must be related to each other.

One common pattern of mixed-fate pedigree involved a mother cell budding three cells in succession (top-right pattern shown in FIGURE 4A). While the mother and the first and the third daughters ultimately activate Wor1, the second daughter does not (FIGURE 4C, 4D, VIDEO 2). With the Wor1-GFP fusion protein, we also observe similar patterns, including an example where a subset of the decedents of the second daughter also activates Wor1 (FIGURE S5). These observations suggest that certain cells undergo a stochastic event that predisposes them and their direct descendents to a higher probability of switching then that observed in the general population. Whether or not cells in these pedigrees actually undergo switching appears to be determined by a second stochastic event. We do not know the basis of the first event (see discussion), but in the next sections, we further explore the second step in which certain cells rapidly increase Wor1 expression.

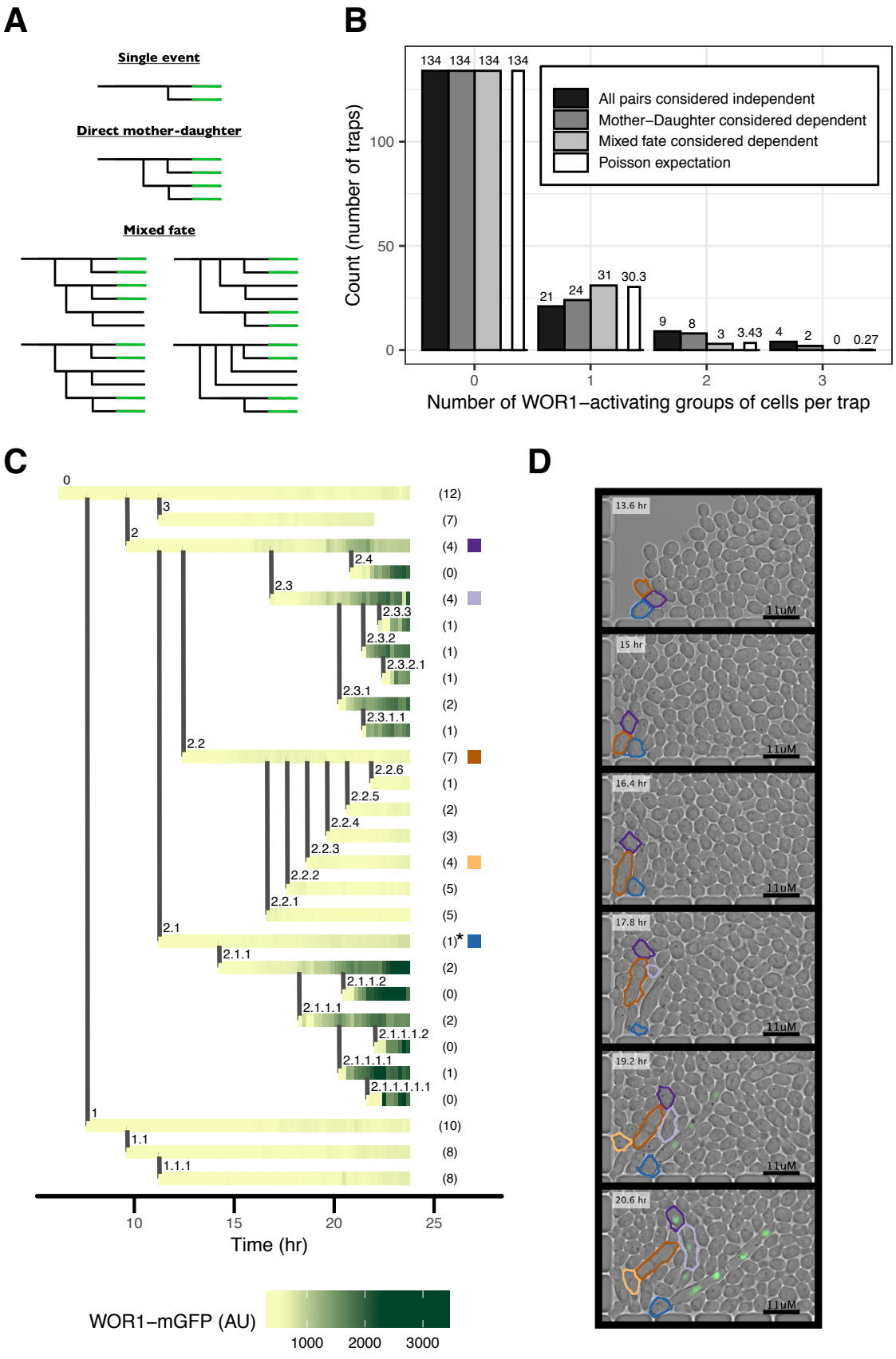

FIGURE 4 legend – Wor1 activation in pedigrees
A) Schematic of pedigree patterns of Wor1 activation, including several examples of mixed-fate pedigrees. Horizontal lines represent single cells; vertical lines represent budding of a daughter cell. Green color represents Wor1 activation. B) Comparison of distributions of the number of switching events per trap to Poisson expectation (white bars). Different distributions are based on including different classes of pedigree patterns as single dependent events. The strain contains the Wor1-mGFP fusion protein. C) Representative mixed-fate pedigree (top-right pattern shown in (A)). Horizontal lines represent single cells; vertical lines represent budding of a daughter cell. Every horizontal line is made up of small tiles representing the measured Wor1-mGFP fluorescence at that time. Numbers within parentheses on the right of the pedigree represent the number of budded daughter cells per cell within the time period shown; not all daughters are depicted in the pedigree. The cell marked by the asterisk lost its nucleus to its daughter cell. Colored square tiles on the right-hand side indicate individual cells that are depicted in (D) using the same color scheme. D) Subset of images representing data shown in (C) with time proceeding from top to bottom. Cell outlines are based on automated image analysis (METHODS).

VIDEO 2 legend – Example of time-lapse movie of a switching event containing a mixed-fate pedigree
Movie corresponds to example in FIGURE 4C. Movie is shown twice; in the second repetition, tracked cells are labeled. This strain contains the Wor1-mGFP fusion protein.

Using a synthetic inducible system in Saccharomyces cerevisiae to investigate the properties of Wor1 autoregulation

Wor1 has been shown to bind to its own control region and to activate its own expression. This positive feedback loop has been proposed to be a critical feature of white-opaque switching (Zordan et al., 2006). Consistent with this hypothesis, we found that the frequency of white-opaque switching is reduced when a single Wor1 motif (out of nine) from the Wor1 control region is deleted (TABLE S1, METHODS). In addition to Wor1, at least 7 other regulators bind the Wor1 control region (Hernday et al., 2013; Lohse & Johnson, 2016), which complicates studying Wor1 autoregulation directly in *C. albicans*. To study Wor1 autoregulation without these confounding factors, we set up the Wor1 autoregulatory loop using a synthetic biology approach (Aranda-Díaz et al., 2017; McIsaac et al., 2014). Specifically, we developed a system in *S. cerevisiae* where we can induce the expression of the *C. albicans* Wor1 protein with progesterone (METHODS, FIGURE 5A) and use flow cytometry to follow the activation of Wor1 transcription using a florescent reporter driven by the *C. albicans* Wor1 regulatory region (METHODS).

The 7KB control region (enhancer) of the *C. albicans* Wor1 was fused to the *S. cerevisiae* Cyc1 core promoter (METHODS) resulting in a reporter that was specifically activated by Wor1 expression (FIGURE S6). Using an mCherry fluorophore for the transcriptional reporter, we created independent (a or α mating type) strains where levels of Wor1, Wor1-GFP, Wor1-mGFP or GFP could be controlled from a synthetic expression construct by adding hormone (METHODS). Comparing Wor1-GFP to Wor1-

mGFP is informative as the ability of GFP to dimerize is the basis for increased switching in *C. albicans* with Wor1-GFP (TABLE S1). As expected, GFP, Wor1-GFP and Wor1-mGFP fluorescence all increased in a hormone dependent manner when driven by the synthetic hormone dependent construct (FIGURE 5B left, FIGURE S7A). Despite identical transcriptional constructs, GFP was induced at ten fold higher levels than Wor1-GFP and Wor1-mGFP (FIGURE 5B left), possibly due to differences in mRNA or protein stability or to translational efficiency. Inducing Wor1 or its GFP fusions also caused physiological effects such as cell clumping, leading to increased autofluorescence (in the Wor1 strains) and bimodal induction distributions (in the Wor1-GFP strains). *S. cerevisiae* has two Wor1 homologs (*MIT1* and *ROF1*) with conserved DNA binding domains and motifs. We created strains where both homologs are deleted and found that the results did not change significantly. We present data for both sets of strains.

Wor1 autoregulation is ultrasensitive and the effect of GFP dimerization informs potential mechanism for increasing switching frequency

The Wor1 transcriptional reporter shows low levels of expression in the absence of hormone (FIGURE S7B). As hormone levels increase, the reporter is activated in strains where the hormone induces Wor1 or its GFP fusions but not when GFP alone is produced (FIGURE5B right). In strains inducing Wor1-GFP and Wor1-mGFP, we could measure both the level of the fusion protein (via the GFP channel) and the response of the Wor1 enhancer (via the mCherry channel) in single cells (FIGURE 5C, FIGURE S8A). To quantify the response function of Wor1 autoregulation, we fit four-parameter log-logistic functions (Hill equations) that describe S-shaped curves, to these distributions (METHODS, FIGURE 5C, 5D). The four parameters specify the lower horizontal asymptote, the upper horizontal asymptote, the value at which the response is half of the maximum and the Hill coefficient, which is a measure of the steepness of the response curve (ultrasensitivity). Hill coefficients greater than 1 imply cooperativity in gene regulation. As reporter expression gradually decreases at high hormone levels in strains containing Wor1-GFP, we only used a subset of conditions for fitting in these strains (METHODS, FIGURE S8A). All curves were ultrasensitive (FIGURE 5D) with mean Hill coefficient estimates of 3.2 (standard deviation, 0.4) for Wor1-mGFP and 4.3 (standard deviation, 0.9) for Wor1-GFP. While there was a small but significant increase in cooperativity for Wor1-GFP over that of Wor1-mGFP (t.test p.value, 0.01), there was a striking difference in the level of protein required for half-max activation, with 5 times higher levels required for Wor1-mGFP than Wor1-GFP (t.test p.value, 8.04e-05). As the ability of GFP to dimerize most likely increases the effective amount of Wor1 found in dimers, the difference in activation thresholds suggests that Wor1 normally acts as a multimer to efficiently bind DNA. Wor1-GFP levels in *C. albicans* opaque cells are comparable to the levels of Wor1-GFP needed to activate the reporter in our synthetic *S. cerevisiae* system (FIGURE S8B), further indicating that the synthetic system captures features of the authentic *C. albicans* circuit.

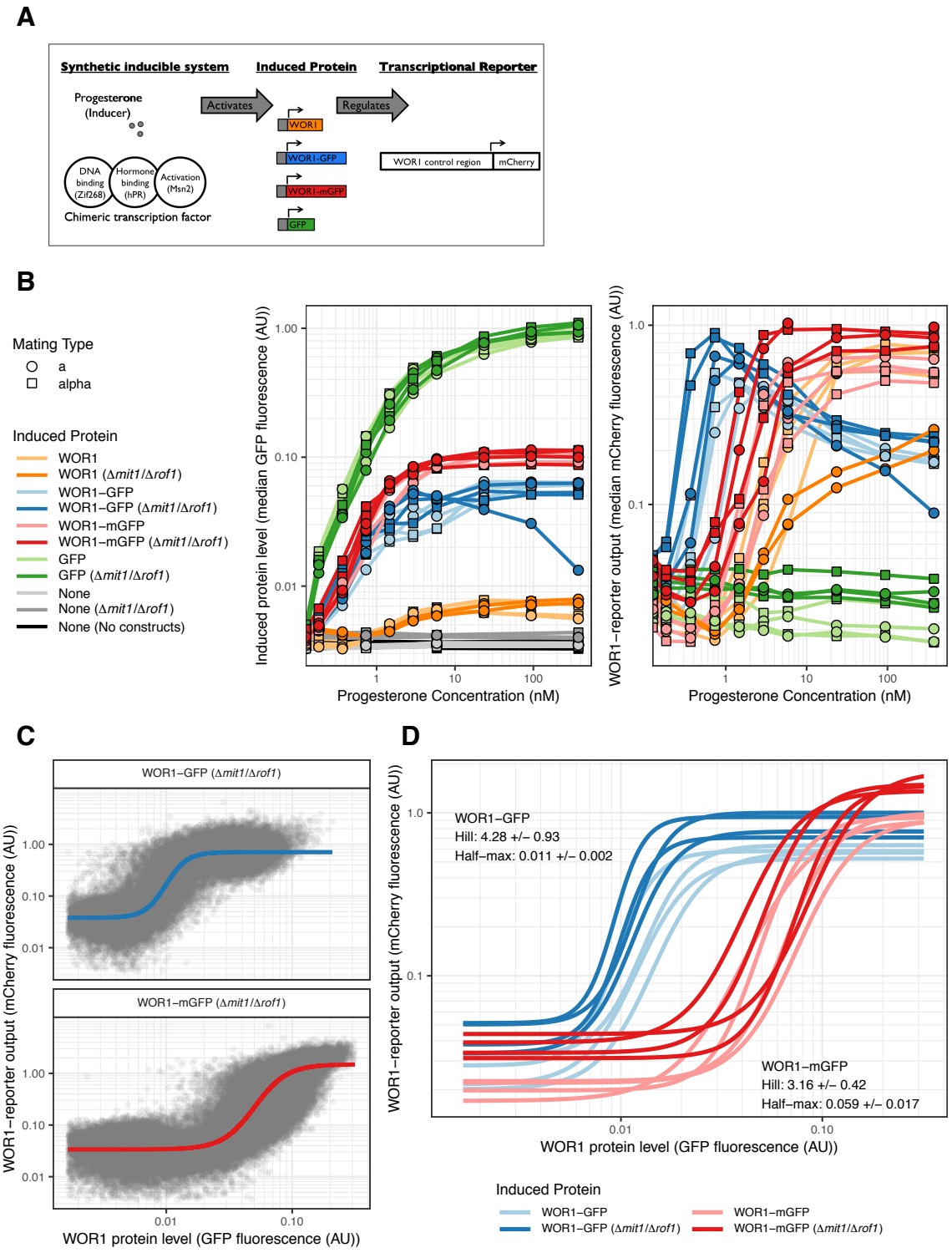

FIGURE 5 legend – Wor1 autoregulation parameters determined by a synthetic inducible system in *Saccharomyces cerevisiae*

A) Schematic of experimental design. B) Median GFP (left) or mCherry (right) fluorescence for strains inducing different proteins in a range of hormone concentrations. Every set of constructs is represented by four independently constructed strains, each measured on two different days (with the exception of the Wor1 (Δ*mit1*/Δ*rof1*) strains which were only measured once). X-axis and Y-axis are logarithmic. C) GFP (Wor1 protein) and mCherry (Wor1 transcriptional activity) fluorescence for individual cells across hormone concentrations. Data is shown for two strains inducing either Wor1-GFP (top) or Wor1-mGFP (bottom) measured on one day. Solid line represents fit Hill equation for each strain. X-axis and Y-axis are logarithmic. D) Fit Hill equation curves for Wor1 transcription activity of strains inducing either Wor1-GFP (blue) or Wor1-mGFP (red). Each curve is fit to data measured on one of two different days. Inset text summarizes parameters for each set of strains (mean +/- standard deviation). X-axis and Y-axis are logarithmic.

Discussion

The ability of cells to switch between different cellular states, each of which are faithfully inherited through many rounds of cell divsion, underlie a wide range of important phenomena including cell differentiation (Sánchez Alvarado & Yamanaka, 2014), antibiotic resistance (Kussell, 2005a; Van den Bergh et al., 2017) and cancer progression (Rosen & Jordan, 2009). The fungal pathogen *Candida albicans* and its close relatives *Candida dubliniensis* and *Candida tropicalis* all undergo a phenomenon known as white-opaque switching, whereby two distinct states are stable across many cell divisions, and switching between them is stochastic (Porman et al., 2011; Pujol et al., 2004). Although this bistable system has been preserved by selection in these species, the mechanism of switching and the complete range of physiological roles of the two cell types are topics of active investigation. It is known that opaque cells are the mating competent cell type (Miller & Johnson, 2002) and are less susceptible to phagocytosis by macrophages, potentially promoting immune evasion (Lohse & Johnson, 2008; Sasse et al., 2013). Recent work has also shown that, due to a specialized secreted protease program, a small number of opaque cells can promote growth of a large white cell population; thus the two cell types can act synergistically (Lohse et al., 2020). Aside from its physiological roles, white-opaque switching has many advantages as a eukaryotic system to study stochastic phenotypic switching. It exemplifies two crucial phenomena, rare stochastic phenotypic switching and cell states that are stable through thousands of cell divisions. It shares many features with bistable networks in multicellular eukaryotes, such as a large number of transcription factors and long, complex regulatory regions (enhancers). White-opaque regulators have also been shown to form phase-separated condensates (Frazer et al., 2020), which are a feature of some mammalian enhancers (Boija et al., 2018). A particular advantage of studying phenotypic switching and heritability in *C. albicans* is the relative ease of performing genetic manipulations. By combining genetic modifications with direct observation of single cells, our goal is to describe in quantitative terms the molecular mechanisms that underlie cell type switching.

Positive feedback, encompassing either positive interactions, double negative interactions, or autocatalysis is necessary, but not sufficient for the creation of bistability (Ferrell, 2002). To facilitate bistability, the response must incorporate non-linearity, also known as ultrasensitivity, in order to create sharp transitions from gradual changes (Ferrell & Ha, 2014). Mechanisms for creating or increasing ultrasensitivity in regulatory responses include cooperative binding of transcriptional regulators (Ackers et al., 1982; Burz, 1998; Johnson et al., 1981), protein sequestration of regulators (Buchler & Cross, 2009) and the number of steps in transcriptional cascades (Hooshangi et al., 2005). We show here that Wor1 regulation of its own promoter is ultrasensitive even in the absence of other *C. albicans* regulators. The propensity to dimerize added by the GFP causes a small increase in the steepness of the activation curve but a large reduction in the activation threshold. It is this large reduction in activation threshold that likely leads to the large increase in white-opaque switching in *C. albicans* cells that harbor Wor1-GFP. This observation suggests switching depends on the equilibrium between Wor1 monomers and higher oligomers. While the natural threshold results in rare switching under standard lab conditions, our results show that switching frequency is easily

adjusted by a relatively small change in the propensity of Wor1 to dimerize. Indeed, other white-opaque regulators may function in a similar manner to the GFP fusion; any increase in Wor1 multimer formation would produce a large effect on switching and could amplify a small amount of Wor1 expression. Although many questions remain concerning the molecular details of Wor1 autoregulation, our results quantify, for the first time, the ultrasensitivity of the WOR1 control region (enhancer) in response to carefully measured levels of the Wor1 protein.

A particular advantage of our study is the use of microfluidics, which has allowed us to observe white-opaque switching at a single cell level and at high temporal resolution. The ability to track single cells and their lineages through time allowed us to make an unexpected observation, that switching can occur in multiple groups of related cells, even when these groups are separated by cell divisions that produce cells that do not switch. The presence of this pattern did not differ between strains containing Wor1-GFP versus Wor1-mGFP despite different switching frequencies. We can draw two conclusions from this switching pattern. First, at least two stochastic events are needed for cells to switch from white to opaque. The first event defines small pedigrees of cells with increased probability of switching and the second event, which only occurs in a subset of cells in these pedigrees, directly leads to Wor1 activation and cell switching. Second, when a complete switching event occurs, several closely related cells in the pedigree switch simultaneously, a property that may be adaptive. The occurrence of coordinated switching would be advantageous in situations where the rapid generation of the rare cell type could be beneficial. For *C. albicans*, increasing the number of opaque cells could be valuable both for immune evasion or metabolic cooperation with white cells. A similar switching pattern was observed in a lab-modified galactose utilization pathway in *Saccharomyces cerevisiae* (Kaufmann et al., 2007). In that study, removal of negative feedback created a system dominated by a single positive feedback loop and led to cells stochastically turning on the GAL regulon in the absence of galactose. In a very similar manner to our observations, the authors saw correlated activation in cell pedigrees, at times separated by cells not activating GAL expression (Kaufmann et al., 2007). This comparison suggests these coordinated switching patterns might be a general feature of eukaryotic bistable systems.

One hypothesis to account for our observed correlations among related cells relies on the stochastic and bursty nature of gene expression (Raj & van Oudenaarden, 2008). According to this hypothesis, the first stochastic event during white-opaque switching might be a rare burst of low-level Wor1 transcription in the absence of efficient translation of Wor1 mRNA. Because no Wor1 is made, this state would be heritable over only a small number of cell divisions, defining the small pedigrees of cells predisposed to switch. The second stochastic event could then depend on variation in translation efficiency (or uneven partitioning during division), with only certain cells in the pedigree accumulating sufficient Wor1 protein to excite the Wor1 positive feedback loop, leading to high level Wor1 expression and subsequent cell-type switching. Consistent with this hypothesis, the Wor1 UTR severely reduces Wor1 protein expression (Guan & Liu, 2015). This hypothesis is subject to explicit testing and will be the focus of future work.

509 Our work has resolved several issues needed for a quantitative molecular understanding
510 of white-opaque switching and lays the foundation for subsequent hypothesis tests. While
511 white-opaque switching and the genetic network that controls it are highly complex, it
512 represents one of only a few cases of a true epigenetic change in a eukaryotic cell that
513 does not require external signals and is simple enough to be analyzed in detail and
514 ultimately, understood in great depth.
515
516

Materials and methods

C. albicans strain construction

The genetic background for *C. albicans* is SC5314. SNY425 was used as a prototrophic a/α reference strain (Noble et al., 2010). For a prototrophic a/Δ reference strain, the α copy of the MTL in SNY250 (Noble & Johnson, 2005) was replaced with a copy of *ARG4* using pJD1 (Lin et al., 2013). Genetic modifications were created using a *SAT1* marker-based CRISPR protocol targeting *Candida maltosa LEU2* (Nguyen et al., 2017). Homozygous Wor1-GFP and Wor1-mGFP fusion proteins were created at the endogenous *WOR1* locus using a combination of two guides encompassing the stop codon (GGTACTTAGTTGAATTAATA and GTACTTAGTTGAATTAATAC). Donor DNA was created by restricting plasmids containing the GFP (or mGFP) sequence flanked by 500 bp of homology to the 3' end of the *WOR1* ORF and 3' UTR (Lohse & Johnson, 2010). The *WOR1* motif deleted from the *WOR1* promoter consists of three overlapping binding motifs (17bp, AAAGTTTAAACTTTAAA), found 5802 bp upstream of the translation start site. A combination of two guides were used for creating the deletion (GAAATTTATGAAAGACGGGT and ACCAGTAGTGATTCATAAAT), donor DNA consisted of 90 bp oligos containing 45 bp homology to flanking sequences with two single bp substitutions to disrupt PAM or guide sequences (AATAATTAGAGTTTTACAAGAAATTTATGAAAGACGGGTGcGAAATACTATA AAATAGAGCAATAAATGACAGAACCTAgCAGTAGTGAT).

S. cerevisiae strain construction

The genetic background for *S. cerevisiae* experiments is S288C. Starting strains were mating type a or α with multiple auxotrophies, created by mating FY23 (*leu2Δ1 ura3-52 trp1Δ63*) (Winston et al., 1995) and a mating type α spore of BY4743 (*his3Δ1 leu2Δ0 lys2Δ0 met15Δ0 ura3Δ0*) (Brachmann et al., 1998). Subsequent transformations integrated various constructs in the following order: the chimeric transcription factor, deletion of the *WOR1* homologs, the induced protein (GFP, Wor1-GFP, Wor1-mGFP or Wor1) and the *WOR1* transcriptional reporter. Plasmids were constructed using either restriction digest and subsequent ligation or by using homology based cloning (In-Fusion, Takara 638911) and were sequence verified, all PCRs utilized a high fidelity polymerase (CloneAmp HiFi PCR Premix, Takara 639298). Plasmids contained components of the synthetic inducible system flanked by homology to the intended genomic integration locus and were restricted prior to transformation. The chimeric transcription factor used is "Z3PM" (Aranda-Díaz et al., 2017) which consists of the Zif268 DNA binding domain, hPR ligand binding domain and the yeast Msn2 activation domain. The transcription factor was expressed from the *S. cerevisiae ADH1* promoter and terminated by the *C. albicans ADH1* terminator. The transcription factor was integrated into *leu2* proceeded by the *Candida glabrata LEU2* sequence, including promoter and terminator. Induced proteins were expressed from a modified *GAL1* promoter containing three dimeric Zif268 binding sites (Aranda-Díaz et al., 2017) and terminated by the *C. albicans ADH1* terminator. The proteins were integrated into the *trp1* locus proceeded by the *C. glabrata TRP1* sequence, including promoter and terminator. The *WOR1* homologs (*MIT1* and *ROF1*) were knocked out using a plasmid based CRISPR approach (Ryan et al., 2014). A plasmid with a 2μ origin of replication was constructed that contained Cas9, a KanMX

selection cassette and two guides (one for each of the homologs). The guides were expressed from the *SNR52* and *SUP4* promoters respectively and both were terminated by a copy of the *SNR52* terminator. Donor DNA consisted of 90bp complementary annealed oligos (Nguyen et al., 2017) containing 44 bp of homology upstream and downstream of the ORF, flanking a GG sequence. After verifying both homologs were deleted, cells were grown overnight in the absence of G418, plated on YPD and replica plated to YPD+G418 to identify colonies that had lost the *CAS9* containing plasmid. The main *WOR1* transcriptional reporter consists of 6656 bp of the *WOR1* promoter (ending at a presumed TATA box, 2048 bp before the translational start site), 115 bp containing the end of the *CYC1* promoter and it's 5' UTR (starting at the "-52" TATA box (Hahn et al., 1985)) and a fluorescent protein ORF (mCherry or GFP) followed by the *C. albicans ACT1* terminator. An alternative reporter contained an additional 70 bp of the end of the *WOR1* promoter and 1980 bp encompassing the *WOR1* 5'UTR instead of the *CYC1* sequence. Transcriptional reporters were preceded by a Hygromycin resistance cassette and integrated into the *ura3* locus. Integration was achieved using two separate restricted plasmids simultaneously transformed. One plasmid contained homology upstream to the *URA3* locus, the Hygromycin cassette and the *WOR1* promoter and beginning of 5' UTR. The second plasmid contained the end of the *WOR1* promoter, the *CYC1* (or *WOR1*) 5'UTR, the florescent protein and terminator and homology downstream to the *URA3* locus. With one exception, combinations of constructs were represented by two completely independent strains based on different starting strains (of mating type a or α). The induced Wor1 (Δ*mit1*/Δ*rof1*) combination was represented by two mating type a strains.

Microscopy and microfluidics

C. albicans strains were streaked from frozen stocks on SD+aa+uri plates and incubated for 5-9 days at 25°C. Colonies were directly diluted to an OD of 0.25 and grown in liquid SD+aa+uri for 4 hours. Cultures were washed and diluted to approximately $5X10^6$ cells/ml in PBS without calcium or magnesium and 50ul were loaded into microfluidic plates. For microfluidic experiments, we used a CellASIC® ONIX microfluidic platform and corresponding Y04T-04 plates. Each plate contains four separate chambers, each chamber containing 104 individual traps. Images were captured using a Nikon Ti2-E microscope equipped with a Photometrics Prime 95B-25mm Camera and a CFI60 Plan Apochromat Lambda 100x Oil immersion objective lens. Cells were loaded into the plate chambers using 55.1 kPa of pressure for 5 seconds and media (SD+aa+uri) flow was started immediately. The media flow program consisted of cycles of three 5 second bursts of perfusion at 10 kPa from each of six inlet channels followed by an hour of perfusion at 1.7 kPa from each of six inlet channels. Coordinates for fields containing single traps loaded with at least one cell were manually determined. Nikon NIS Elements software was used to drive stage movement and acquisition; the Nikon Perfect Focus System was utilized. Images (DIC and GFP channels) were captured for each field (40-70 per chamber) every 12 minutes for 24 hours. Temperature was kept at 25°C using an OKOLab Cage Incubator.

Image and data analysis

Custom Matlab scripts were used for image analysis; statistical analysis and data visualization utilized R (R Core Team, 2019), with extensive use of *tidyverse* (Wickham, 2017). Images were first adjusted to correct for stage movement. Each image was compared to the previous image in the time series and the optimal geometric transformation was found to account for any (x,y) movement (Matlab function *imregtform*). Next, cells were segmented automatically in each image. Cell borders were identified using a combination of bottom hat filtering, top hat filtering, dilation, erosion and selection based on object properties (area, perimeter and eccentricity). Individual cells were tracked through time by manually determining their position in a series of images; each position was then associated with the corresponding automatically segmented cell. Pedigree information was also manually determined. For a metric of Wor1 expression per cell, the 300 highest intensity pixels (in the GFP channel) were averaged. Typical white cell size is 1,750 pixels; typical opaque cell size is 2,500 pixels. Cell length (FIGURE 2, FIGURE S2) was determined using Fiji (Schindelin et al., 2012) by recording the length of a line drawn along the cells long axis. Cell length was recorded when cells were beginning to bud a new cell. 100 reference white and opaque cells were recorded. Cell length was recorded for all pairs of switching cells across three experiments from different days, resulting in 248 mother-daughter pairs of cells containing Wor1-GFP and 50 pairs of cells containing Wor1-mGFP. For determining if mixed-fate pedigrees represent two independent switching events, we considered 168 traps loaded with cells containing Wor1-mGFP. The numbers of switching events were counted in each trap according to three different ways of calculating independent events: 1) every pair of mother-daughter cells are considered independent, 2) pairs of direct mother-daughter pairs are no longer considered independent, 3) pairs in mixed-fate pedigrees are also no longer considered independent. We calculated the expected Poisson probability distribution based on the unambiguous zero-class of 134 traps (λ=-log(134/168)). We performed chi-squared goodness-of-fit tests with p-values computed by Monte Carlo simulations with 2000 replicates.

Flow cytometry, experiments and data analysis

S. cerevisiae strains were streaked from frozen stocks on YPD plates and incubated for 2 days at 30°C. Colonies were inoculated into 3ml of SD+aa+uri media and grown overnight. Cells were washed, resuspended in PBS without calcium or magnesium and diluted 1:16 into 96-well plates containing SD+aa+uri with different concentrations of progesterone. Progesterone was diluted from 2mM stocks (95% Ethanol, 5% DMSO); lower concentrations were supplemented with Ethanol and DMSO to match the high concentration. Plates contained 8 experimental strains measured at 10 different concentrations of progesterone and 3 control strains measured at 4 concentrations of progesterone. For each set of strains two identical plates were created and incubated, shaking at 500 RPM at 30°C. After a set incubation time, plates were washed three times and diluted in PBS without calcium or magnesium with 1mM EDTA. One plate was read after 4.5 hours of incubation and the second was read at 24 hours. Data from both plates were similar and the 24-hour readings are presented. Measurements were taken using a BD FACSCelesta. GFP fluorescence was measured by blue (488nm) excitation and a 530/30 band pass emission filter. mCherry fluorescence was measured by yellow-green

(561nm) excitation and a 610/20 band pass emission filter. Flow cytometery data was analyzed using R (R Core Team, 2019), with extensive use of *tidyverse* (Wickham, 2017). Data was imported into R using *flowCore* (Ellis et al., 2019). Data was filtered to remove potential cell debris, cell aggregates and contaminants by constructing two gates, one based on forward and side scatter and a second based on GFP and a violet (405nm) excitation, 670/30 emission channel. GFP and mCherry measurements were normalized by forward scatter. Presented data encompass 376 wells with a range of 127-8905 events per well after filtering (median: 7095.5; 95% of samples have over 4000 events). For fitting hill equations, we used the *drm* function in the package *drc* (Ritz et al., 2015) using robust median estimation. mCherry measurements were log10 transformed and fitted to a four-parameter log-logistic function with a parameterization converting the natural log of the half-max value into a parameter. For Wor1-GFP, only data from progesterone concentrations less than 2nM were used for fitting.

Acknowledgments

We thank members of the Johnson lab, in particular Matt Lohse and Kyle Fowler for helpful discussions and Ananda Mendoza for technical support. We thank David Gresham, Kerry Geiler-Samerotte, Mariana Gomez Schiavon and Ranen Aviner for advice and the lab of Hana El-Samad and Dmitri Petrov for providing reagents. This investigation has been aided by a grant from The Jane Coffin Childs Memorial Fund for Medical Research (to N.Z.).

678 References
679

680 Acar, M., Mettetal, J. T., & van Oudenaarden, A. (2008). Stochastic switching as a
681 survival strategy in fluctuating environments. *Nature Genetics*, *40*(4), 471–475.
682 https://doi.org/10.1038/ng.110
683 Ackers, G. K., Johnson, A. D., & Shea, M. A. (1982). Quantitative model for gene
684 regulation by lambda phage repressor. *Proceedings of the National Academy of*
685 *Sciences*, *79*(4), 1129–1133. https://doi.org/10.1073/pnas.79.4.1129
686 Alon, U. (2007). Network motifs: Theory and experimental approaches. *Nature Reviews*
687 *Genetics*, *8*(6), 450–461. https://doi.org/10.1038/nrg2102
688 Aranda-Díaz, A., Mace, K., Zuleta, I., Harrigan, P., & El-Samad, H. (2017). Robust
689 Synthetic Circuits for Two-Dimensional Control of Gene Expression in Yeast.
690 *ACS Synthetic Biology*, *6*(3), 545–554. https://doi.org/10.1021/acssynbio.6b00251
691 Bergen, M. S., Voss, E., & Soll, D. R. (1990). Switching at the cellular level in the
692 white—Opaque transition of Candida albicans. *Journal of General Microbiology*,
693 *136*(10), 1925–1936. https://doi.org/10.1099/00221287-136-10-1925
694 Boija, A., Klein, I. A., Sabari, B. R., Dall'Agnese, A., Coffey, E. L., Zamudio, A. V., Li,
695 C. H., Shrinivas, K., Manteiga, J. C., Hannett, N. M., Abraham, B. J., Afeyan, L.
696 K., Guo, Y. E., Rimel, J. K., Fant, C. B., Schuijers, J., Lee, T. I., Taatjes, D. J., &
697 Young, R. A. (2018). Transcription Factors Activate Genes through the Phase-
698 Separation Capacity of Their Activation Domains. *Cell*, *175*(7), 1842-1855.e16.
699 https://doi.org/10.1016/j.cell.2018.10.042
700 Brachmann, C. B., Davies, A., Cost, G. J., Caputo, E., Li, J., Hieter, P., & Boeke, J. D.
701 (1998). Designer deletion strains derived from Saccharomyces cerevisiae S288C:

A useful set of strains and plasmids for PCR-mediated gene disruption and other applications. *Yeast (Chichester, England)*, *14*(2), 115–132. https://doi.org/10.1002/(SICI)1097-0061(19980130)14:2<115::AID-YEA204>3.0.CO;2-2

Buchler, N. E., & Cross, F. R. (2009). Protein sequestration generates a flexible ultrasensitive response in a genetic network. *Molecular Systems Biology*, *5*(1), 272. https://doi.org/10.1038/msb.2009.30

Burz, D. S. (1998). Cooperative DNA-binding by Bicoid provides a mechanism for threshold-dependent gene activation in the Drosophila embryo. *The EMBO Journal*, *17*(20), 5998–6009. https://doi.org/10.1093/emboj/17.20.5998

Çağatay, T., Turcotte, M., Elowitz, M. B., Garcia-Ojalvo, J., & Süel, G. M. (2009). Architecture-Dependent Noise Discriminates Functionally Analogous Differentiation Circuits. *Cell*, *139*(3), 512–522. https://doi.org/10.1016/j.cell.2009.07.046

Chickarmane, V., Troein, C., Nuber, U. A., Sauro, H. M., & Peterson, C. (2006). Transcriptional Dynamics of the Embryonic Stem Cell Switch. *PLoS Computational Biology*, *2*(9), e123. https://doi.org/10.1371/journal.pcbi.0020123

Ellis, B., Haaland, P., Hahne, F., Meur, N. L., Gopalakrishnan, N., Spidlen, J., Jiang, M., & Finak, G. (2019). *FlowCore: FlowCore: Basic structures for flow cytometry data*.

Ene, I. V., Lohse, M. B., Vladu, A. V., Morschhäuser, J., Johnson, A. D., & Bennett, R. J. (2016). Phenotypic Profiling Reveals that *Candida albicans* Opaque Cells Represent a Metabolically Specialized Cell State Compared to Default White

725 Cells. *MBio*, *7*(6), e01269-16, /mbio/7/6/e01269-16.atom.
726 https://doi.org/10.1128/mBio.01269-16
727 Ferrell, J. E. (2002). Self-perpetuating states in signal transduction: Positive feedback,
728 double-negative feedback and bistability. *Current Opinion in Cell Biology*, *14*(2),
729 140–148. https://doi.org/10.1016/S0955-0674(02)00314-9
730 Ferrell, J. E., & Ha, S. H. (2014). Ultrasensitivity part III: Cascades, bistable switches,
731 and oscillators. *Trends in Biochemical Sciences*, *39*(12), 612–618.
732 https://doi.org/10.1016/j.tibs.2014.10.002
733 Frazer, C., Staples, M. I., Kim, Y., Hirakawa, M., Dowell, M. A., Johnson, N. V.,
734 Hernday, A. D., Ryan, V. H., Fawzi, N. L., Finkelstein, I. J., & Bennett, R. J.
735 (2020). Epigenetic cell fate in Candida albicans is controlled by transcription
736 factor condensates acting at super-enhancer-like elements. *Nature Microbiology*,
737 *5*(11), 1374–1389. https://doi.org/10.1038/s41564-020-0760-7
738 Gardner, T. S., Cantor, C. R., & Collins, J. J. (2000). Construction of a genetic toggle
739 switch in Escherichia coli. *Nature*, *403*(6767), 339–342.
740 https://doi.org/10.1038/35002131
741 Graham, T. G. W., Tabei, S. M. A., Dinner, A. R., & Rebay, I. (2010). Modeling bistable
742 cell-fate choices in the Drosophila eye: Qualitative and quantitative perspectives.
743 *Development*, *137*(14), 2265–2278. https://doi.org/10.1242/dev.044826
744 Guan, Z., & Liu, H. (2015). The *WOR 1* 5′ untranslated region regulates white-opaque
745 switching in *Candida albicans* by reducing translational efficiency: *WOR1* 5′
746 untranslated region. *Molecular Microbiology*, *97*(1), 125–138.
747 https://doi.org/10.1111/mmi.13014

748 Hahn, S., Hoar, E. T., & Guarente, L. (1985). Each of three "TATA elements" specifies a
749 subset of the transcription initiation sites at the CYC-1 promoter of
750 Saccharomyces cerevisiae. *Proceedings of the National Academy of Sciences of*
751 *the United States of America*, *82*(24), 8562–8566.
752 Hernday, A. D., Lohse, M. B., Fordyce, P. M., Nobile, C. J., DeRisi, J. L., & Johnson, A.
753 D. (2013). Structure of the transcriptional network controlling white-opaque
754 switching in *Candida albicans*. *Molecular Microbiology*, *90*(1), 22–35.
755 https://doi.org/10.1111/mmi.12329
756 Hooshangi, S., Thiberge, S., & Weiss, R. (2005). Ultrasensitivity and noise propagation
757 in a synthetic transcriptional cascade. *Proceedings of the National Academy of*
758 *Sciences*, *102*(10), 3581–3586. https://doi.org/10.1073/pnas.0408507102
759 Johnson, A. D., Poteete, A. R., Lauer, G., Sauer, R. T., Ackers, G. K., & Ptashne, M.
760 (1981). λ Repressor and cro—Components of an efficient molecular switch.
761 *Nature*, *294*(5838), 217–223. https://doi.org/10.1038/294217a0
762 Kaufmann, B. B., Yang, Q., Mettetal, J. T., & van Oudenaarden, A. (2007). Heritable
763 Stochastic Switching Revealed by Single-Cell Genealogy. *PLoS Biology*, *5*(9),
764 e239. https://doi.org/10.1371/journal.pbio.0050239
765 Kim, J., & Sudbery, P. (2011). Candida albicans, a major human fungal pathogen. *The*
766 *Journal of Microbiology*, *49*(2), 171–177. https://doi.org/10.1007/s12275-011-
767 1064-7
768 Kramer, B. P., Viretta, A. U., Baba, M. D.-E., Aubel, D., Weber, W., & Fussenegger, M.
769 (2004). An engineered epigenetic transgene switch in mammalian cells. *Nature*
770 *Biotechnology*, *22*(7), 867–870. https://doi.org/10.1038/nbt980

771 Kussell, E. (2005a). Bacterial Persistence: A Model of Survival in Changing
772 Environments. *Genetics*, *169*(4), 1807–1814.
773 https://doi.org/10.1534/genetics.104.035352
774 Kussell, E. (2005b). Phenotypic Diversity, Population Growth, and Information in
775 Fluctuating Environments. *Science*, *309*(5743), 2075–2078.
776 https://doi.org/10.1126/science.1114383
777 Lin, C.-H., Kabrawala, S., Fox, E. P., Nobile, C. J., Johnson, A. D., & Bennett, R. J.
778 (2013). Genetic Control of Conventional and Pheromone-Stimulated Biofilm
779 Formation in Candida albicans. *PLoS Pathogens*, *9*(4), e1003305.
780 https://doi.org/10.1371/journal.ppat.1003305
781 Lohse, M. B., Brenes, L. R., Ziv, N., Winter, M. B., Craik, C. S., & Johnson, A. D.
782 (2020). An Opaque Cell-Specific Expression Program of Secreted Proteases and
783 Transporters Allows Cell-Type Cooperation in *Candida albicans*. *Genetics*,
784 genetics.303613.2020. https://doi.org/10.1534/genetics.120.303613
785 Lohse, M. B., Ene, I. V., Craik, V. B., Hernday, A. D., Mancera, E., Morschhauser, J.,
786 Bennett, R. J., & Johnson, A. D. (2016). Systematic Genetic Screen for
787 Transcriptional Regulators of the Candida albicans White-Opaque Switch.
788 *Genetics*, *203*(4), 1679–1692. https://doi.org/10.1534/genetics.116.190645
789 Lohse, M. B., & Johnson, A. D. (2008). Differential phagocytosis of white versus opaque
790 Candida albicans by Drosophila and mouse phagocytes. *PloS One*, *3*(1), e1473.
791 https://doi.org/10.1371/journal.pone.0001473

792 Lohse, M. B., & Johnson, A. D. (2009). White–opaque switching in Candida albicans.
793 *Current Opinion in Microbiology*, *12*(6), 650–654.
794 https://doi.org/10.1016/j.mib.2009.09.010
795 Lohse, M. B., & Johnson, A. D. (2010). Temporal anatomy of an epigenetic switch in cell
796 programming: The white-opaque transition of C. albicans. *Molecular*
797 *Microbiology*, *78*(2), 331–343. https://doi.org/10.1111/j.1365-2958.2010.07331.x
798 Lohse, M. B., & Johnson, A. D. (2016). Identification and Characterization of Wor4, a
799 New Transcriptional Regulator of White-Opaque Switching. *G3:*
800 *Genes|Genomes|Genetics*, *6*(3), 721–729. https://doi.org/10.1534/g3.115.024885
801 Losick, R., & Desplan, C. (2008). Stochasticity and Cell Fate. *Science*, *320*(5872), 65–68.
802 https://doi.org/10.1126/science.1147888
803 Maamar, H., & Dubnau, D. (2005). Bistability in *the Bacillus subtilis* K-state
804 (competence) system requires a positive feedback loop: Bistability in *B. subtilis*
805 competence. *Molecular Microbiology*, *56*(3), 615–624.
806 https://doi.org/10.1111/j.1365-2958.2005.04592.x
807 McIsaac, R. S., Gibney, P. A., Chandran, S. S., Benjamin, K. R., & Botstein, D. (2014).
808 Synthetic biology tools for programming gene expression without nutritional
809 perturbations in Saccharomyces cerevisiae. *Nucleic Acids Research*, *42*(6), e48–
810 e48. https://doi.org/10.1093/nar/gkt1402
811 Miller, M. G., & Johnson, A. D. (2002). White-opaque switching in Candida albicans is
812 controlled by mating-type locus homeodomain proteins and allows efficient
813 mating. *Cell*, *110*(3), 293–302.

814 Nguyen, N., Quail, M. M. F., & Hernday, A. D. (2017). An Efficient, Rapid, and
815 Recyclable System for CRISPR-Mediated Genome Editing in *Candida albicans*.
816 *MSphere*, *2*(2). https://doi.org/10.1128/mSphereDirect.00149-17
817 Noble, S. M., French, S., Kohn, L. A., Chen, V., & Johnson, A. D. (2010). Systematic
818 screens of a Candida albicans homozygous deletion library decouple
819 morphogenetic switching and pathogenicity. *Nature Genetics*, *42*(7), 590–598.
820 https://doi.org/10.1038/ng.605
821 Noble, S. M., & Johnson, A. D. (2005). Strains and Strategies for Large-Scale Gene
822 Deletion Studies of the Diploid Human Fungal Pathogen *Candida albicans*.
823 *Eukaryotic Cell*, *4*(2), 298–309. https://doi.org/10.1128/EC.4.2.298-309.2005
824 Norman, T. M., Lord, N. D., Paulsson, J., & Losick, R. (2015). Stochastic Switching of
825 Cell Fate in Microbes. *Annual Review of Microbiology*, *69*(1), 381–403.
826 https://doi.org/10.1146/annurev-micro-091213-112852
827 Park, B. O., Ahrends, R., & Teruel, M. N. (2012). Consecutive Positive Feedback Loops
828 Create a Bistable Switch that Controls Preadipocyte-to-Adipocyte Conversion.
829 *Cell Reports*, *2*(4), 976–990. https://doi.org/10.1016/j.celrep.2012.08.038
830 Phillips, G. N. (1997). Structure and dynamics of green fluorescent protein. *Current*
831 *Opinion in Structural Biology*, *7*(6), 821–827. https://doi.org/10.1016/S0959-
832 440X(97)80153-4
833 Porman, A. M., Alby, K., Hirakawa, M. P., & Bennett, R. J. (2011). Discovery of a
834 phenotypic switch regulating sexual mating in the opportunistic fungal pathogen
835 Candida tropicalis. *Proceedings of the National Academy of Sciences*, *108*(52),
836 21158–21163. https://doi.org/10.1073/pnas.1112076109

837 Ptashne, M. (2011). Principles of a switch. *Nature Chemical Biology*, *7*(8), 484–487.
838 https://doi.org/10.1038/nchembio.611
839 Pujol, C., Daniels, K. J., Lockhart, S. R., Srikantha, T., Radke, J. B., Geiger, J., & Soll,
840 D. R. (2004). The Closely Related Species Candida albicans and Candida
841 dubliniensis Can Mate. *Eukaryotic Cell*, *3*(4), 1015–1027.
842 https://doi.org/10.1128/EC.3.4.1015-1027.2004
843 R Core Team. (2019). *R: A Language and Environment for Statistical Computing*. R
844 Foundation for Statistical Computing. https://www.R-project.org/
845 Raj, A., & van Oudenaarden, A. (2008). Nature, Nurture, or Chance: Stochastic Gene
846 Expression and Its Consequences. *Cell*, *135*(2), 216–226.
847 https://doi.org/10.1016/j.cell.2008.09.050
848 Ritz, C., Baty, F., Streibig, J. C., & Gerhard, D. (2015). Dose-Response Analysis Using
849 R. *PLOS ONE*, *10*(12), e0146021. https://doi.org/10.1371/journal.pone.0146021
850 Rosen, J. M., & Jordan, C. T. (2009). The Increasing Complexity of the Cancer Stem Cell
851 Paradigm. *Science*, *324*(5935), 1670–1673.
852 https://doi.org/10.1126/science.1171837
853 Ryan, O. W., Skerker, J. M., Maurer, M. J., Li, X., Tsai, J. C., Poddar, S., Lee, M. E.,
854 DeLoache, W., Dueber, J. E., Arkin, A. P., & Cate, J. H. (2014). Selection of
855 chromosomal DNA libraries using a multiplex CRISPR system. *ELife*, *3*, e03703.
856 https://doi.org/10.7554/eLife.03703
857 Sánchez Alvarado, A., & Yamanaka, S. (2014). Rethinking Differentiation: Stem Cells,
858 Regeneration, and Plasticity. *Cell*, *157*(1), 110–119.
859 https://doi.org/10.1016/j.cell.2014.02.041

860 Santillán, M., & Mackey, M. C. (2008). Quantitative approaches to the study of
861 bistability in the *lac* operon of *Escherichia coli*. *Journal of The Royal Society*
862 *Interface*, *5*(suppl_1). https://doi.org/10.1098/rsif.2008.0086.focus
863 Sasse, C., Hasenberg, M., Weyler, M., Gunzer, M., & Morschhauser, J. (2013). White-
864 Opaque Switching of Candida albicans Allows Immune Evasion in an
865 Environment-Dependent Fashion. *Eukaryotic Cell*, *12*(1), 50–58.
866 https://doi.org/10.1128/EC.00266-12
867 Schindelin, J., Arganda-Carreras, I., Frise, E., Kaynig, V., Longair, M., Pietzsch, T.,
868 Preibisch, S., Rueden, C., Saalfeld, S., Schmid, B., Tinevez, J.-Y., White, D. J.,
869 Hartenstein, V., Eliceiri, K., Tomancak, P., & Cardona, A. (2012). Fiji: An open-
870 source platform for biological-image analysis. *Nature Methods*, *9*(7), 676–682.
871 https://doi.org/10.1038/nmeth.2019
872 Smits, W. K., Kuipers, O. P., & Veening, J.-W. (2006). Phenotypic variation in bacteria:
873 The role of feedback regulation. *Nature Reviews Microbiology*, *4*(4), 259–271.
874 https://doi.org/10.1038/nrmicro1381
875 Stockwell, S. R., Landry, C. R., & Rifkin, S. A. (2015). The yeast galactose network as a
876 quantitative model for cellular memory. *Molecular BioSystems*, *11*(1), 28–37.
877 https://doi.org/10.1039/C4MB00448E
878 Sudbery, P., Gow, N., & Berman, J. (2004). The distinct morphogenic states of Candida
879 albicans. *Trends in Microbiology*, *12*(7), 317–324.
880 https://doi.org/10.1016/j.tim.2004.05.008
881 Tuch, B. B., Mitrovich, Q. M., Homann, O. R., Hernday, A. D., Monighetti, C. K., De La
882 Vega, F. M., & Johnson, A. D. (2010). The Transcriptomes of Two Heritable Cell

883 Types Illuminate the Circuit Governing Their Differentiation. *PLoS Genetics*,
884 *6*(8), e1001070. https://doi.org/10.1371/journal.pgen.1001070
885 Van den Bergh, B., Fauvart, M., & Michiels, J. (2017). Formation, physiology, ecology,
886 evolution and clinical importance of bacterial persisters. *FEMS Microbiology*
887 *Reviews*, *41*(3), 219–251. https://doi.org/10.1093/femsre/fux001
888 Wernet, M. F., Mazzoni, E. O., Çelik, A., Duncan, D. M., Duncan, I., & Desplan, C.
889 (2006). Stochastic spineless expression creates the retinal mosaic for colour
890 vision. *Nature*, *440*(7081), 174–180. https://doi.org/10.1038/nature04615
891 Wickham, H. (2017). *tidyverse: Easily Install and Load the "Tidyverse."*
892 https://CRAN.R-project.org/package=tidyverse
893 Winston, F., Dollard, C., & Ricupero-Hovasse, S. L. (1995). Construction of a set of
894 convenientsaccharomyces cerevisiae strains that are isogenic to S288C. *Yeast*,
895 *11*(1), 53–55. https://doi.org/10.1002/yea.320110107
896 Wu, M., Su, R.-Q., Li, X., Ellis, T., Lai, Y.-C., & Wang, X. (2013). Engineering of
897 regulated stochastic cell fate determination. *Proceedings of the National Academy*
898 *of Sciences*, *110*(26), 10610–10615. https://doi.org/10.1073/pnas.1305423110
899 Yang, F., Moss, L. G., & Phillips, G. N. (1996). The molecular structure of green
900 fluorescent protein. *Nature Biotechnology*, *14*(10), 1246–1251.
901 https://doi.org/10.1038/nbt1096-1246
902 Zacharias, D. A. (2002). Partitioning of Lipid-Modified Monomeric GFPs into
903 Membrane Microdomains of Live Cells. *Science*, *296*(5569), 913–916.
904 https://doi.org/10.1126/science.1068539

905 Zordan, R. E., Galgoczy, D. J., & Johnson, A. D. (2006). Epigenetic properties of white-
906 opaque switching in Candida albicans are based on a self-sustaining
907 transcriptional feedback loop. *Proceedings of the National Academy of Sciences*,
908 *103*(34), 12807–12812. https://doi.org/10.1073/pnas.0605138103
909 Zordan, R. E., Miller, M. G., Galgoczy, D. J., Tuch, B. B., & Johnson, A. D. (2007).
910 Interlocking Transcriptional Feedback Loops Control White-Opaque Switching in
911 Candida albicans. *PLoS Biology*, *5*(10), e256.
912 https://doi.org/10.1371/journal.pbio.0050256
913
914

White to Opaque switching

Genotype	Plates	Colonies	Sectors	Percent Switch	Fold Change
WT	11 (3,3,5)	1340	17	1.27 (+/- 0.306)	-
Wor1 motif deletion	11 (3,3,5)	1790	8	0.447 (+/- 0.158)	2.83 down
Wor1-GFP	11 (3,3,5)	948	491	51.8 (+/- 1.62)	40.8 up
Wor1-mGFP	11 (3,3,5)	1603	31	1.93 (+/- 0.344)	1.52 up

Opaque to White switching

Genotype	Plates	Colonies	Sectors	Percent Switch	Fold Change
WT	11 (3,3,5)	1926	87	4.52 (+/- 0.473)	-
Wor1 motif deletion	11 (3,3,5)	1159	224	19.3 (+/- 1.16)	4.28 up
Wor1-GFP	11 (3,3,5)	1633	0	<0.06	>75 down
Wor1-mGFP	11 (3,3,5)	1707	52	3.05 (+/- 0.42)	1.48 down

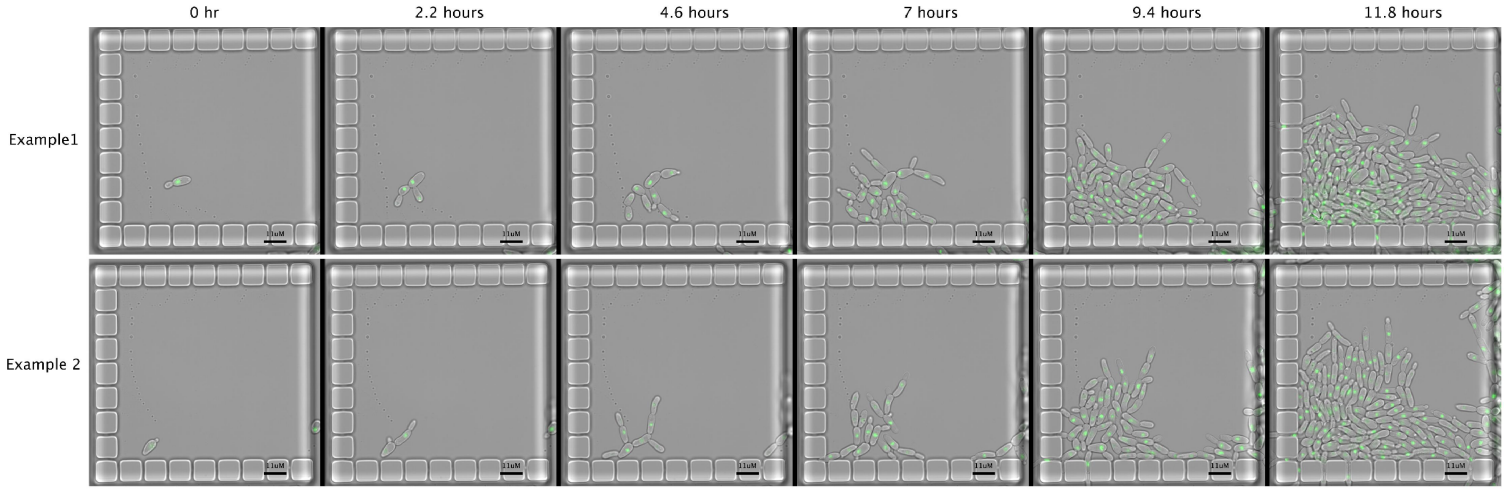

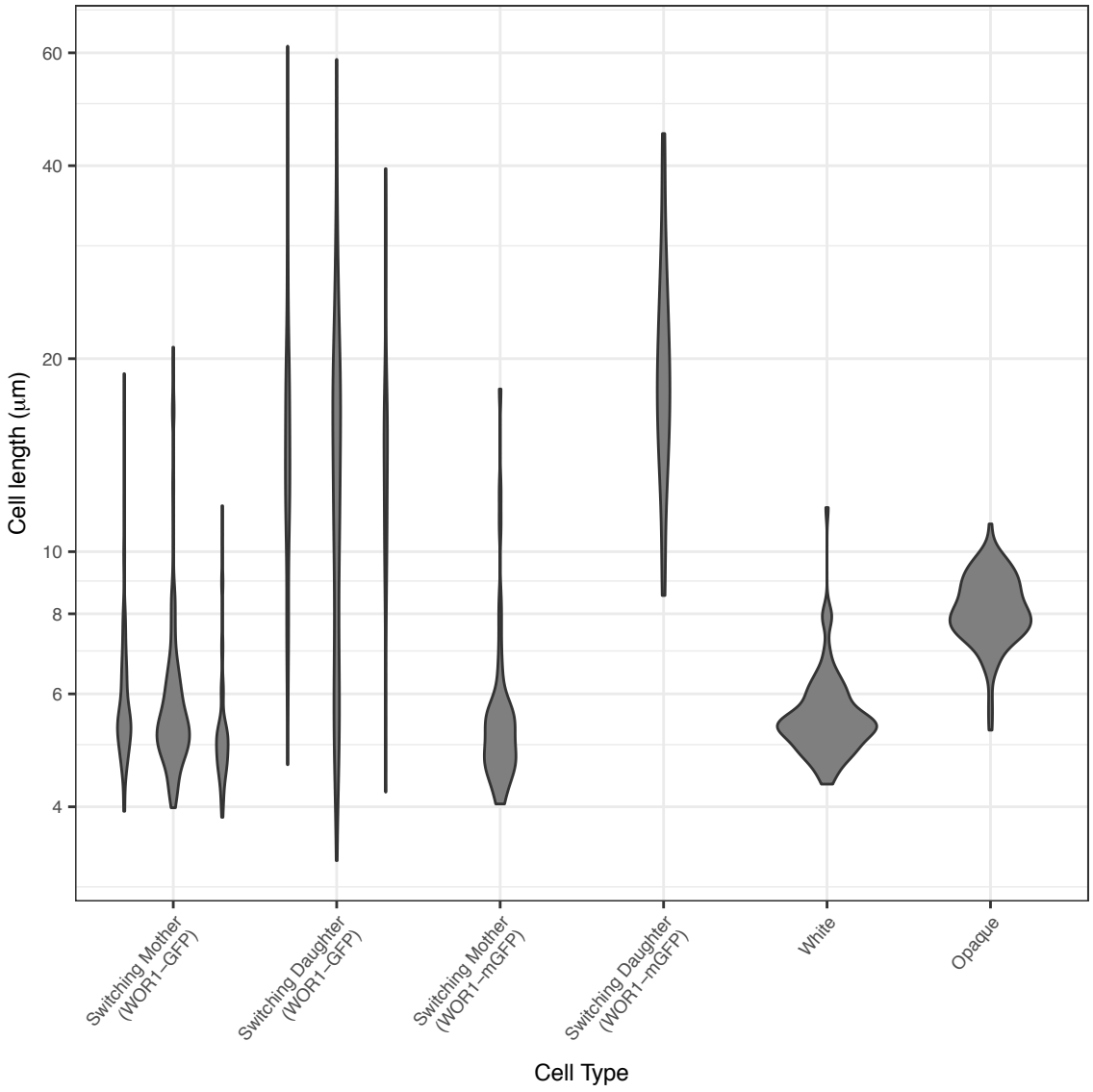

A

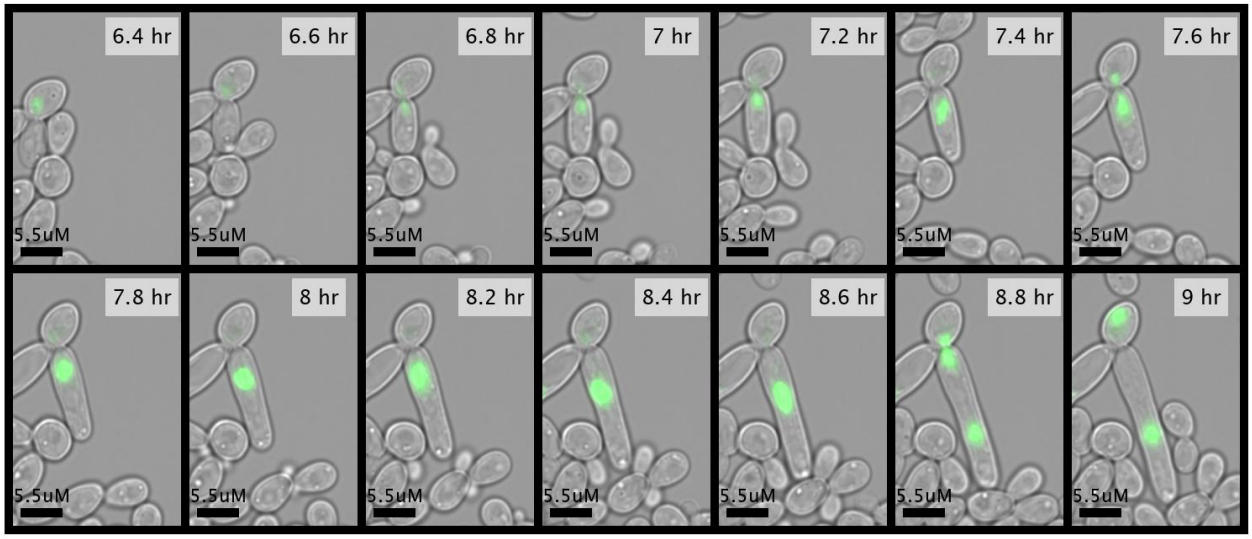

B